

Contents lists available at ScienceDirect

Computers in Biology and Medicine

journal homepage: www.elsevier.com/locate/compbiomed



Thickness profile of the ganglion cell complex and choroid in patients with persistent diabetic macular edema



Ana Condelipes ^a, Daniela Correia ^a, Inês Fernandes ^a, Tiago Silva ^a, Eduardo Correia ^b, Bruno Pereira ^{a,c,d}

D. Pedro Camacho ^{a,d,e,*}

- ^a H&TRC- Health & Technology Research Center, ESTeSL- Escola Superior de Tecnologia da Saúde, Instituto Politécnico de Lisboa, Lisbon, Portugal
- ^b Instituto Superior de Ciências do Trabalho e da Empresa, ISCTE, Lisbon, Portugal
- ^c iNOVA4Health, NOVA Medical School, Faculdade de Cièncias Médicas, NMS, FCM, Universidade NOVA de Lisboa, Lisbon, Portugal
- ^d Instituto de Retina de Lisboa, IRL, Lisbon, Portugal
- ^e ULS São José, Lisbon, Portugal

ARTICLE INFO

Keywords:
Diabetes mellitus
Diabetic macular edema
Diabetic retinopathy
Ganglion cell complex
Choroid
SD-OCT

ABSTRACT

Purpose: About 40 % of patients with diabetic macular edema (DME) do not respond optimally to first-line treatment with intravitreal injection of anti-vascular endothelial growth factor (AVEGF). Evidence suggests that additional vascular and neurodegenerative mechanisms may be involved. This study aimed to characterise the thickness of the Ganglion Cell Complex (GCC) and investigate the Choroidal Vascularity Index (CVI) in patients with different patterns of therapeutic response to AVEGF DME.

Methods: This cross-sectional study included 27 diabetic patients into 3 different groups based on their response to AVEGF therapy: control group, responder DME group, and persistent DME group. The study's approach to vascular and neurodegenerative imaging biomarkers involved three steps: (1) Automatic quantification of GCC thickness, with manual correction when necessary; (2) Semi-automatic measurement of choroidal thickness; and (3) Analysis of choroidal area and choroidal luminal area using ImageJ software to calculate the CVI.

Results: In the overall characterization of the sample, a significant difference was observed only in the Best Corrected Visual Acuity (BCVA). There was a significant difference in Average Retinal Thickness (1 mm, 3 mm, and 6 mm) between the 3 groups and in GCC thickness at 1 mm. BCVA was negatively correlated with mean retinal thickness, while CVI showed a potential positive correlation with BCVA.

Conclusions: While demographic and general clinical characteristics showed minimal differences across the groups, important differences in GCC and choroidal characteristics were observed. GCC (1 mm) may be interesting to explore in predicting visual outcomes after treatment, and CVI may impact visual gain.

1. Introduction

The global prevalence of Diabetes Mellitus (DM) has progressively increased over the past decades, with projections suggesting it will reach approximately 643 million by 2030 [1]. This growth is expected to lead to an increase in macrovascular and microvascular complications such as Diabetic Retinopathy (DR). Traditionally, studies have focused on vascular dysfunction and the resulting microvascular lesions; however, recent research has highlighted the role of retinal neurodegeneration as a process that may precede microangiopathy [2–7], as well as the contribution of inflammation, which affects both vascular integrity and neuronal function in the diabetic retina [14].

The first-line treatment for Diabetic Macular Edema (DME), the leading cause of vision loss in patients with DR, involves intravitreal injection of anti-vascular endothelial growth factor (AVEGF), providing significant functional and structural improvements. However, multicenter studies show that nearly 40 % of patients do not respond well to AVEGF therapy [8–10].

Various studies have been conducted to understand the different therapeutic responses. Genetic evaluation, epigenetic, and metabolomic studies have explored compromised pathways [11–13]. Neural apoptosis, glial activation, and oxidative stress are the main mechanisms of retinal neurodegeneration described in DM, affecting the inner retinal layers, particularly the Ganglion Cell Layer [14].

^{*} Corresponding author. ESTeSL – Escola Superior de Tecnologia da Saúde de Lisboa, Av. D. João II, Lote 4.69.01, 1990-096, Lisbon, Portugal. E-mail address: pedro.camacho@estesl.ipl.pt (P. Camacho).

Inflammation is a complex biological process involving multiple cell types and chemical mediators. In the context of diabetic retinopathy, it represents a non-infectious chronic response triggered by hyperglycaemia-induced oxidative stress and excitotoxicity. These factors activate retinal glial cells, which release pro-inflammatory cytokines and chemokines that contribute to both vascular dysfunction and neurodegeneration [9,10,14].

Consequently, due to the highly complex pathogenesis and the involvement of various biochemical pathways, such as neuro-inflammation, cellular permeability alteration, and retinal cell apoptosis [4], some patients exhibit persistent DME even after months of AVEGF therapy [25]. Recognising these cases is essential not only to predict treatment response, but also to guide therapeutic decisions, including potential need for switching to alternative or adjunctive therapies targeting inflammatory mechanisms.

Early identification and characterisation of retinal structural patterns may therefore be crucial for anticipating and monitoring therapeutic response, and for determining when a change in treatment strategy is warranted [15]. The integrity of retinal ganglion cells, which play a key role in preserving visual function, also appears to be clinically relevant [4], as their profile has been associated with primary neuro-degeneration, retinal ischemia, and potential toxicity related to intravitreal agents [16].

Variations in choroidal thickness in patients with DME have been studied, with increases linked to inflammatory mechanisms and decreases associated with ischemic components [17]. However, accurately quantifying the choroid is challenging due to the reliance on automatic algorithms, and its relationship with the therapeutic response to AVEGF treatment remains unclear [18].

In this context, the present study aims to build upon previous research that primarily focused on differences in DNA methyltransferase gene expression among patients with varying DME response patterns [11]. This study seeks to complement previous work by examining classical imaging biomarkers obtained through Optical Coherence Tomography (OCT), which were not previously explored. Specifically, it aims to characterise Ganglion Cell Complex (GCC) thickness and choroidal thickness in DME patients with different AVEGF therapeutic response patterns. Additionally, having some choroidal features, it also evaluates the Choroidal Vascularity Index (CVI) in this cohort, as changes in CVI may be associated with hypoxia in the retinal pigment epithelium (RPE) and outer retinal layers, potentially leading to increased secretion of vascular endothelial growth factor (VEGF) [19].

2. Materials and methods

This study employed a cross-sectional approach based on the original data from the DiffMeDiME study (IDI&CA grant IPL/2021/DiffMeDiME_ESTeSL) [11] conducted at the Escola Superior de Tecnologia da Saúde de Lisboa (ESTeSL) in collaboration with Instituto Retina de Lisboa (IRL) and Associação Protetora dos Diabéticos de Portugal (APDP).

The primary objective of the main study was to describe differences in the DNA methyltransferase gene expression in patients with different patterns of response to DME. However, crucial traditional imaging biomarkers obtained through OCT were not explored. To complement the main project, this present study aimed to quantify the GCC and choroid thickness in patients with DME and different therapeutic response patterns to AVEGF.

This study was approved by the Ethics Committee of the ESTeSL (CE-ESTeSL-No.08-2021) and the Ethics Committees of the IRL and APDP. All procedures and data acquisition conducted during the study adhered to the principles of the Declaration of Helsinki. A detailed explanation of the study objectives was provided to each participant, and informed written consent was obtained freely and consciously.

3. Selection and classification of patients

Using a non-probabilistic convenience sample, 27 Type 2 Diabetes Mellitus (T2DM) patients from IRL and APDP clinical practice with fluorescein angiography (FA) assessment supporting the clinical diagnosis were included in this study. Given the difficulty in identifying good responders and cases of persistent DME in the early stages of treatment, only patients who had undergone a minimum of three consecutive monthly intravitreal injections of ranibizumab (Lucentis®) and had at least six months of clinical follow-up were included [20]. Patients were not treatment-naïve at inclusion, as all were under active anti-VEGF therapy. Previous focal/grid laser or anti-VEGF therapy prior to this treatment regimen were not exclusion criteria, reflecting a real-world clinical cohort. Therapeutic response was classified according to criteria adapted from the Diabetic Retinopathy Clinical Research Network (DRCR.net) Protocol I, as detailed in a previous publication [11]. Based on their response to AVEGF treatment, patients were divided into three groups: control group (CG, n = 11), responder DME group (DMEr, n = 9), and persistent DME group (DMEp, n = 7). The classification of Diabetic Retinopathy was performed independently by two experienced evaluators according to the Early Treatment Diabetic Retinopathy Study (ETDRS) classification.

3.1. Inclusion criteria

- DMEr Group: Patients with DME (central retinal thickness \geq 305 µm in women and \geq 320 µm in men), with a thickness reduction >10 % on SD-OCT [21,22] and an early BCVA response (\geq 5 letters) in the study eye [24].
- DMEp Group: Patients with persistent DME (central retinal thickness ≥305 µm in women and ≥320 µm in men), with stable/worsening/ improvement <10 % on SD-OCT at least 180 days after treatment and suboptimal BCVA response (<5 letters) in the study eye [23,25].
- Control Group: Patients of the same age, diabetic but without DR.
 This group consists of individuals who visited the IRL for a general ophthalmology consultation.

Exclusion criteria: uncontrolled systemic disease, intraocular pressure (IOP) > 21 mmHg and/or suspicious RNFL changes, presence of AMD, glaucoma or vitreomacular pathology in the study eye, high ametropia (SE greater than -6.00 D and +2.00D), diabetic macular ischemia (as identified by FA), systemic disease affecting the eyes, and a history of heart disease.

One eye per patient was included in the analysis, corresponding to the eye undergoing AVEGF treatment at the time of inclusion. Eligible participants had undergone a comprehensive ophthalmological examination, including best-corrected visual acuity (BCVA) assessment using the ETDRS scale, ultra-widefield color fundus photography (133°) with the Clarus 500® system (Carl Zeiss Meditec), and spectral-domain optical coherence tomography (SD-OCT) using the Spectralis® platform (Heidelberg Engineering). Additionally, clinical and demographic data such as age, duration of diabetes mellitus, and glycated hemoglobin (HbA1c) levels were collected for each participant.

3.2. Quantitative assessment by spectral-domain OCT

The SD-OCT acquisition protocol consisted of obtaining a macular volume scan (High-density SD-OCT raster volume scan), which includes acquisitions of $20^{\circ} \times 20^{\circ}$, 49 horizontal high-resolution B-scans (raster with 1024 A-scans per B-scan with a depth resolution of 3.9 μm , mean of 7 frames per scan) centered on the fovea. For choroidal analysis, an additional high-resulution scan centered on the fovea was acquired using the same volume scan protocol but with enhanced depth imaging (EDI) mode activated. Choroidal thickness and CVI measurements were derived from these EDI scans, while retinal and GCC measurements were based on first macular volume protocol.

For this study, data acquisition regarding the thickness of the Retina, Ganglion Cell Layer, Inner Plexiform Layer, and other layers were obtained through segmentation performed on all 49 B-scans by the SD-OCT Spectralis (Heidelberg Engineering®). All measurements across the 1323 B-scans were obtained automatically, with manual corrections applied whenever necessary to ensure precision. In cases where doubts persisted in analyzing certain B-scans, the final segmentation decisions were thoroughly reviewed and confirmed by two independent experts (BP and PC).

3.3. Ganglion cell complex

Each layer was evaluated according to the values obtained in the ETDRS grid (9 sectors, 4 quadrants). The thickness of the GCC was obtained by summing the thickness values of the Ganglion Cell Layer (obtained between the inner margin of the Nerve Fiber Layer and the inner boundary of the Inner Plexiform Layer) and the Inner Plexiform Layer (obtained between the outer margin of Ganglion Cell Layer and the inner boundary of Inner Nuclear Layer) in the 9 sectors of the ETDRS grid [24].

3.4. Quantification of choroidal thickness

Choroidal segmentation was performed semi-automatically following the protocol by Zhao et al. [25] minimising manual intervention. This method has demonstrated excellent inter-observer reproducibility in previous studies (intraclass correlation coefficient, ICC = 0.976). The analysis was applied across all 49 B-scans and involved the following three sequential steps: first, the overall retinal thickness (ILM-BM) was measured using the built-in segmentation algorithm of the Spectralis OCT system; second, the retina-choroid thickness was measured by manually adjusting the reference line from BM to the posterior boundary of the choroid, finally, the choroidal thickness was obtained by subtracting the overall retinal thickness (ILM-BM) from the retina-choroid thickness (ILM-choroidoscleral interface) for all ETDRS sectors [26]. Given the complexity of these measurements, rigorous procedures were implemented to ensure accuracy and minimize variability. Two masked senior researchers in retinal imaging (PC and BP) reviewed all B-scans in a blinded manner to correct any segmentation errors or decentration prior to analysis. A standardized protocol, consistent with prior studies [27] and with identical segmentation approaches [28], was followed to mitigate potential biases introduced by manual corrections. In addition, interobserver agreement was assessed using intraclass correlation coefficients (ICC) across ETDRS sectors (see Supplementary Material 7).

To minimize diurnal and environmental variability, all SD-OCT assessments were performed between 9:00 a.m. and 12:00 p.m., after a 30-min rest period. During this time, patients avoided physical activity and were exposed to controlled ambient lighting to reduce luminance and accommodation-related fluctuations.

3.5. Choroidal Vascularity Index (CVI) assessment

The CVI is an innovative parameter that allows for the assessment of the vascular state of the choroid, which is associated with the integrity of the RPE and VEGF secretion. It may be relevant in evaluating the vascular state of the choroid by quantifying the luminal and stromal components through the ratio between the choroidal luminal area and the total choroidal area [19].

For the study of CVI, the B-scan centered on the fovea was selected to perform the choroid analysis, following the protocol described by Sonoda et al. [29] with some modifications.

Binarization in the OCT image is a technique that converts grayscale images into binarized images, facilitating the analysis of irregular illumination, contrast variation, and low resolution. This was done using the Niblack method, which converts grayscale tones into black and

white based on neighboring pixels. The Niblack method converted the image from RGB format (red, blue, green) (Fig. 1A) to 8-bit format (Fig. 1B) to obtain a clear view of the choroid-scleral interface, using a class originated in Java (version 1.8.0.391) [30].

The RGB format image was processed with ImageJ software (version 1.54g; public domain, provided by the National Institutes of Health, Bethesda, MD, USA https://imagej.net/ij/), where the total choroidal area was initially manually selected using the Polygon tool. The entire B-scan was used to segment the total choroidal area, which was then entirely converted to red to calculate the total choroidal area in pixels.

ImageJ software allows converting the binarized 8-bit image to RGB format without altering the image, which is necessary to select the area of light pixels corresponding to the choroidal luminal area. This was calculated by combining the segmented total choroidal area image with the binarized RGB image (Fig. 1C). The stromal area, corresponding to dark pixels, was calculated by subtracting the luminal area from the choroidal area. Subsequently, the unit of measurement was converted from pixels to square millimeters. Using the screen size and resolution of the computer, the pixels per inch were calculated, allowing for the calculation of pixels per millimeter (ppm). This enables a formula that requires the area in pixels and the ppm (area in pixels/ppmm²) to obtain the result in mm². The binarized image was combined with the segmented total choroidal area image with the RGB format image, obtaining outlined areas that coincide with the choroidal luminal area (Fig. 1D) [31].

4. Statistical analysis

The collected data were analyzed using the Statistical Package for the Social Sciences (IBM SPSS 27). Initially, descriptive statistical analysis was conducted. For this purpose, the mean and standard deviation were calculated for continuous variables and relative frequencies for the categorical variables.

Subsequently, either the Chi-square test or Fisher's exact test was applied to categorical variables, depending on the expected cell frequencies, to assess statistically significant differences between groups. For quantitative variables, the normality of the sample was evaluated using the Shapiro-Wilk test. Based on the results, ANOVA or Kruskal-Wallis tests were applied as appropriate to compare group means. Furthermore, a Multivariate Analysis of Variance (MANOVA) was conducted to evaluate significant differences across the defined groups for two dependent variables simultaneously. When significant differences were identified, Spearman's correlation test and scatter plots were utilized to explore relationships between variables. Statistical significance was set at $\rm p < 0.05$.

4.1. Statistical power analysis and Effect Size Calculation

To assess the adequacy of statistical power for detecting statistically significant differences, post-hoc power analyses were conducted for key metrics in the study: GCC thickness, retina thickness, choroid area, choroid vascular area, and CVI. The calculations included the following steps.

- Effect Size Calculation: Effect sizes were calculated for comparisons across the three groups using ANOVA, and Cohen's dd was applied for post-hoc pairwise comparisons.
- ii) ii) Power Calculation: Statistical power was estimated using the noncentrality parameter for the F-distribution in ANOVA.

To ensure precision and reproducibility, Python 3.10 with the SciPy library was utilized for these post-hoc analyses, including effect size and power calculations.

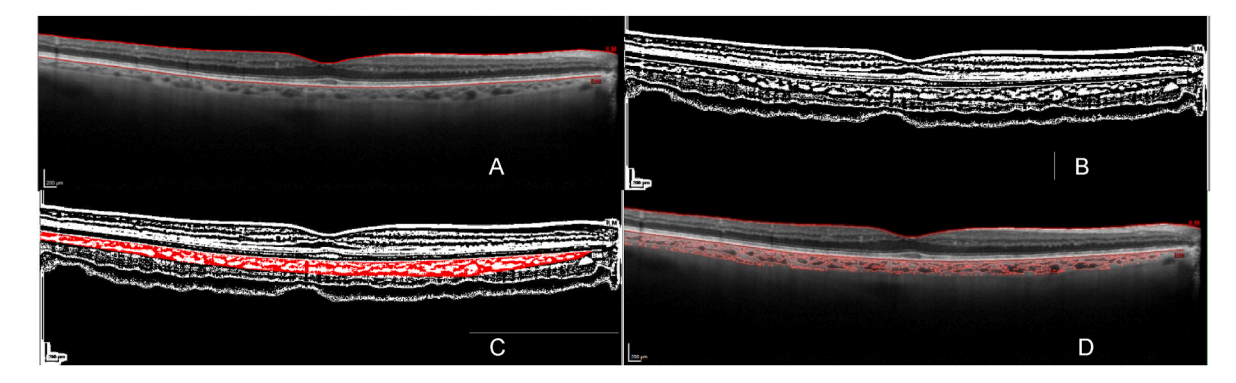


Fig. 1. Choroidal image binarization in an eye Belonging to the responder group.

Legend: Original SD-OCT image (A) was converted using the image binarization approach (B). Combination of the total choroidal area segmentation image and the binarized image (C). Overlay of the region of interest, created after image binarization, on the SD-OCT image (D).

5. Results

The sample consisted of 27 patients, of which 55.6 % were female, and 44.4 % were male, with an average age of 71.6 \pm 7.9 years. The patients were classified into three groups: the Control Group (CG), consisting of 11 individuals (40.7 %); the DMEr Group, consisting of 9 individuals (33.3 %); and the DMEp Group, consisting of 7 individuals (25.9 %).

Table 1 shows a significant decrease in BCVA (p < 0.001) among the studied groups. The Control Group (CG) showed BCVA (81.9 \pm 2.6 letters) compared to the DMEr group (68.6 \pm 8.8 letters) and DMEp group (59.0 \pm 13.4 letters). No statistically significant differences were found among the groups for the remaining parameters.

A significant difference in DR classification was observed among groups (p < 0.001). All participants in the Control group had no DR or minimal NPDR, while both DMEr and DMEp groups presented comparable distributions across DR severity levels.

Table 2 presents the main differences observed in retinal layers. In the GCL, it was observed that the DMEp group $(24.3\pm4.5\,\mu\text{m})$ showed a statistically significant increase in mean thickness at the central 1 mm (p < 0.001) compared to the other groups (DMEr group - $18.2\pm6.0\,\mu\text{m}$; CG - $13.5\pm2.0\,\mu\text{m}$). Multiple comparisons in GCL (1 mm ETDRS) revealed significant differences between CG – DMEr (p = 0.050) and CG – DMEp (p < 0.001) groups. A similar pattern of increased mean thickness was also found in GCL (3 mm ETDRS), where the DMEp group (47.7 \pm 9.6 μm) exhibited greater mean thickness than other groups. Significant differences were found between CG – DMEr (p = 0.042) and CG – DMEp (p < 0.001) in this segmentation.

In the INL, statistically significant differences were found at 1 mm (p = 0.006) and 6 mm (p = 0.050). In INL (1 mm ETDRS), the DMEr group (37.6 \pm 15.4 μ m) showed greater mean thickness than the other groups.

The most significant differences in mean thickness of INL (1 mm ETDRS) were found between CG – DMEr (p=0.010) and CG – DMEp (p=0.006) groups, while in INL (6 mm ETDRS) significant difference was only observed between CG – DMEr (p=0.026) group.

In OPL, significant differences were found at 3 mm (p = 0.009) and 6 mm (p = 0.044), indicating an increase in thickness in the DMEp group (37.9 \pm 5.7 $\mu m)$ and DMEr group (30.4 \pm 2.8 $\mu m)$, respectively. Significant differences were observed at 3 mm between CG – DMEr (p = 0.010) and CG – DMEp (p = 0.013) groups, while at 6 mm, a significant difference was observed only between CG – DMEr (p = 0.013) groups.

In ONL, the DMEr group (98.9 \pm 24.7 μ m) showed a statistically significant increase in mean thickness at the central 1 mm (p = 0.022), with a significant difference observed between DMEr – DMEp (p = 0.006).

Regarding the retinal thickness, the DMEp group showed a significant increase in thickness at 1 mm (p < 0.001), 3 mm (p < 0.001), and 6 mm (p = 0.024) compared to the CG and DMEr groups. Multiple comparisons revealed statistically significant differences in Retina (1 mm ETDRS) between CG – DMEr (p = 0.034) and CG – DMEp (p < 0.001), in Retina (3 mm ETDRS) between CG – DMEr (p = 0.013) and CG – DMEp (p < 0.001), and in Retina (6 mm ETDRS) between CG – DMEr (p = 0.016) and CG – DMEp (p = 0.031).

In Table 3, it was observed that despite the absence of differences in the traditional approach to choroidal thickness quantification, statistically significant differences were found in the Choroidal Area (p < 0.001) and Choroidal Vascular Area (p < 0.001). Regarding the Choroidal Area, the CG ($10.4\pm7.9~\text{mm}^2$) exhibited a larger area than the other groups. Statistical analysis between groups showed significant differences between CG – DMEr (p = 0.006) and DMEr – DMEp (p = 0.024), where CG had a larger area ($10.4\pm7.9~\text{mm}^2$) and DMEr had a smaller area ($3.0\pm1.0~\text{mm}^2$). As for the Choroidal Vascular Area, CG

Table 1
Demographic and clinical characteristics of the sample by groups.

		Control Group $n=11$ (40.7 %)	DMEr Group $n=9$ (33.3 %)	DMEp Group $n=7$ (25.9 %)	p-value	
Age (years) $\overline{x} \pm SD$		74.3 ± 6.8	69.8 ± 7.3	69.7 ± 9.9	0.355	
Sex n (%)	Female	5 (45.5 %)	4 (44.4 %)	6 (85.7 %)	0.175	
	Male	6 (54.5 %)	5 (55.6 %)	1 (14.3 %)		
BCVA (score) $\bar{x} \pm SD$		81.9 ± 2.6	68.6 ± 8.8	59.0 ± 13.4	<.001	
Spherical equivalent (D) $\bar{x} \pm SD$		0.47 ± 0.42	0.42 ± 0.87	0.36 ± 0.69	0.980	
DM duration (years) $\bar{x} \pm SD$		18.3 ± 6.2	22.2 ± 10.4	21.7 ± 10.8	0.642	
DR Classification n (%)	No DR or minimal NPDR	11 (100 %)	1 (11.1 %)	0 (0 %)	<.001	
	Mild NPDR	0 (0 %)	1 (11.1 %)	1 (16.7 %)		
	Intermediate NPDR	0 (0 %)	1 (11.1 %)	1 (16.7 %)		
	Severe NPDR	0 (0 %)	6 (66.7 %)	4 (66.7 %)		
IOP (mmHg) $\overline{x} \pm SD$		15.0 ± 0.8	15.0 ± 1.6	16 ± 2.6	0.183	

Legend: DM = Diabetes Mellitus; F = female; D = dioptre; SD = standard deviation; BCVA = Best Corrected Visual Acuity; n/a = not applicable; PIO = intraocular pressure; DR = Diabetic Retinopathy; NPDR = Non-Proliferative Diabetic Retinopathy. Statistically significant values are highlighted in bold in Table 1 (p < 0.05).

Table 2
Average thickness (μm) of retinal layers in the sample by groups.

	- 1	Control Group		DMEp Group	p-Value
GCL (μm) x̄ ± SD	1 mm	13.5 ± 2.0	18.2 ± 6.0	24.3 ± 4.5	<.001**
x ± 3D	3	48.1 ± 4.4	46.4 ± 5.4	51.3 ± 4.5	0.150
	mm 6	34.9 ± 2.9	35.3 ± 4.5	35.4 ± 2.9	0.957
IPL (μm) \overline{x}	mm 1	18.6 ± 2.1	22.4 ± 6.2	23.4 ± 6.0	0.098
\pm SD	mm 3	39.7 ± 3.3	39.6 ± 3.2	44.7 ± 7.9	0.432
	mm 6	29.2 ± 2.8	30.6 ± 2.8	31.5 ± 2.1	0.204
GCC (μ m) $\overline{x} \pm SD$	mm 1 mm	32.2 ± 3.2	40.7 ± 12.1	47.7 ± 9.6	.003**
A ± 3D	3 mm	87.8 ± 7.7	86.1 ± 8.1	96.0 ± 10.3	0.071
	6 mm	64.2 ± 5.7	65.8 ± 7.1	66.9 ± 4.4	0.613
INL (μm) \overline{x}	1 mm	20.0 ± 4.3	31.9 ± 9.1	37.6 ± 15.4	.006**
\pm SD	3 mm	40.5 ± 5.1	44.7 ± 5.2	49.3 ± 10.4	0.090
	6 mm	32.1 ± 2.4	35.7 ± 3.2	35.0 ± 4.4	.050*
OPL (μ m) $\bar{x} \pm SD$	1 mm	24.1 ± 5.2	25.1 ± 4.1	31.1 ± 9.3	0.070
	3 mm	31.1 ± 3.7	37.5 ± 5.6	37.9 ± 5.7	.009**
	6 mm	26.6 ± 1.6	30.4 ± 2.8	29.0 ± 4.4	.044*
ONL (μ m) $\bar{x} \pm SD$	1 mm	96.0 ± 8.2	98.9 ± 24.7	$\textbf{77.7} \pm \textbf{17.2}$.022#
	3 mm	70.8 ± 10.0	81.3 ± 17.4	75.6 ± 8.1	0.201
	6 mm	56.7 ± 7.4	69.3 ± 14.1	61.4 ± 10.4	0.062
Retina $(\mu m) \overline{x}$	1 mm	266.2 ± 15.4	328.1 ± 69.3	428.3 ± 81.3	<.001**
± SD	3 mm	330.6 ± 18.9	358.1 ± 18.4	387.8 ± 35.0	<.001**
	6 mm	294.3 ± 18.3	321.8 ± 26.3	322.9 ± 28.9	.024**
RNFL (μ m) $\bar{x} \pm SD$		102.8 ± 10.0	98.8 ± 9.6	102.6 ± 8.0	0.427

Legend: GCL = Ganglion Cell Layer; GCC = Ganglion cel layer complex; ppRNFL = Peri-papilar Retinal Nerve Fiber Layer; ONL = Outer Nuclear Layer; INL = Inner Nuclear Layer; OPL = Outer Plexiform Layer; IPL = Inner Plexiform Layer; SD = Standard Deviation. The values of Retinal Layer Thickness are presented as mean $(\bar{x}) \pm Standard$ Deviation. Statistically significant values are highlighted in bold in Table 2 (p \leq 0.05). Symbols (*; ***; #) in Table 2 indicate statistically significant differences (p \leq 0.05) obtained through Bonferroni correction for multiple comparisons across different groups (*CG – DMEr; ** CG – DMEr and CG – DMEp; # DMEr- DMEp). Details of the multiple correlations can be found in Annex 1.

also exhibited a larger area ($5.5 \pm 4.9 \text{ mm}^2$) than the other groups. Multiple comparisons revealed significant differences between CG – DMEr (p = 0.012) and DMEr – DMEp (p = 0.031), with CG having a larger area ($5.5 \pm 4.9 \text{ mm}^2$) and DMEr ($1.4 \pm 4.5 \text{ mm}^2$) showing a smaller area. Choroidal thickness measurements obtained independently by the two investigators, as well as the corresponding intraclass correlation coefficients (ICC) across ETDRS sectors, are provided in Supplementary Material 7.

5.1. Correlation between BCVA and ganglion cell complex

To evaluate the presence of statistically significant differences between the different groups (CG, DMEr, and DMEp) regarding two dependent variables (BCVA and Average Thickness of the Ganglion Cell Complex), a Multivariate Analysis of Variance (Manova) was conducted. This statistical analysis was performed for both Average Thicknesses of the Ganglion Cell Complex (1 mm, 3 mm, and 6 mm), revealing a significant difference in the correlation between BCVA and the Thickness of the Ganglion Cell Complex among the 3 groups in the 1 mm ETDRS (p < 0.001), 3 mm ETDRS (p < 0.001), and 6 mm ETDRS (p = 0.002). Considering the significant differences in the correlation between these two variables among the 3 groups, Spearman's Correlation coefficient was calculated to correlate BCVA with the Thickness of the Ganglion Cell Complex in different sectors (Fig. 2). A moderate negative correlation

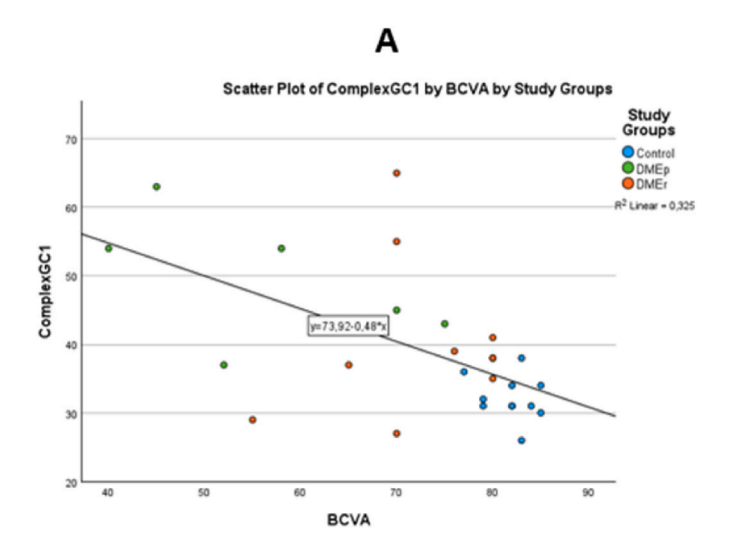


Fig. 2. Scatter plot of BCVA and average thickness of the ganglion cell complex (1 mm).

Legend: Control = Control Group; BCVA = Best-Corrected Visual Acuity; ComplexGC1 = Average Thickness of the Ganglion Cell Complex (1 mm); Fig. 2 depicts the simple linear regression between BCVA and the Thickness of the Ganglion Cell Complex (A - 1 mm).

Table 3
Characteristics of Vascular Area (mm²), Choroidal Vascularity index and Choroidal Thickness (μm).

		Control Group	DMEr Group	DMEp Group	p-value
Choroidal Area (mm ²) $\overline{x} \pm SD$		10.4 ± 7.9	3.0 ± 1.0	7.0 ± 3.8	<.001**
Choroidal Vascular Area (mm ²) $\overline{x} \pm SD$		5.5 ± 4.9	1.4 ± 4.5	3.1 ± 1.7	<.001##
Choroidal Vascularity Index (%) $\overline{x} \pm SD$		49 ± 8	43 ± 3	44 ± 2	0.201
Choroidal Thickness (μ m) $\overline{x} \pm SD$	1 mm	287.0 ± 143.9	221.7 ± 66.3	214.7 ± 71.8	0.553
	3 mm	286.5 ± 139.8	227.6 ± 65.7	236.8 ± 42.1	0.729
	6 mm	260.4 ± 114.1	206.9 ± 60.2	213.6 ± 40.2	0.597

Legend: SD = Standard Deviation; Values for Choroidal Area, Choroidal Vascular Area, Choroidal Vascularity Index, and Choroidal Thickness are presented as mean (\bar{x}) \pm Standard Deviation. Statistically significant values are highlighted in bold in Table 3 (p \leq 0.05). Symbols (##) in Table 3 indicate statistically significant differences (p \leq 0.05) obtained by Bonferroni correction for multiple comparisons across different groups (## CG- DMEr and DMEr- DMEp). Further details on multiple correlations can be found in Annex 1.

was found in the 1 mm ETDRS (r = -0.515; p = 0.03). The remaining correlations (3 mm and 6 mm) can be found in Annex 3.

5.2. BCVA and retinal thickness

To assess the presence of significant differences among the different groups (CG, DMEr, and DMEp) regarding two dependent variables (BCVA and Average Retinal Thickness), a Multivariate Analysis of Variance (ANOVA) was conducted. This statistical analysis was performed for both Average Retinal Thicknesses (1 mm, 3 mm, and 6 mm), revealing significant differences in the correlation between BCVA and Average Retinal Thickness among the three groups at 1 mm ETDRS (p < 0.001), 3 mm ETDRS (p < 0.001), and 6 mm ETDRS (p < 0.001). Given the significant differences found in the correlation of these two variables among the three groups, Spearman's Correlation Coefficient was used to correlate BCVA with Retinal Thickness in different sectors (Fig. 3), revealing a moderate negative correlation at 1 mm ETDRS (r = -0.504; p = 0.004), 3 mm ETDRS (r = -0.693; p < 0.001), and on 6 mm ETDRS (r = -0.504; p = 0.004).

5.3. Correlation between BCVA and CVI

To assess significant differences among the different groups (CG, DMEr, and DMEp) regarding two dependent variables (BCVA and CVI), a Multivariate Analysis of Variance (ANOVA) was conducted. Significant differences were found in the correlation between BCVA and CVI across the three groups (p < 0.001). Subsequently, Spearman's correlation coefficient was used to assess the correlation between BCVA and CVI. BCVA did not show a statistically significant correlation with CVI (p = 0.057). The Spearman's correlation coefficient value (r = 0.312) suggests a potential positive correlation between BCVA and CVI (Annex 4).

5.4. Correlation between BCVA and choroidal area

To assess significant differences among the different groups (CG, DMEr, and DMEp) regarding two dependent variables (BCVA and Choroidal Area), a Multivariate Analysis of Variance (Manova) was conducted. Significant differences were found in the correlation between BCVA and Choroidal Area across the three groups (p < 0.001). Considering the significant difference observed, Spearman's correlation coefficient was used to assess the correlation between BCVA and Choroidal Area (r = 0.124; p = 0.269). These two variables' correlations were not statistically significant (Annex 5).

5.5. Correlation between BCVA and choroidal vascular area

To assess significant differences among the different groups (CG, DMEr, and DMEp) regarding two dependent variables (BCVA and Choroidal Vascular Area), a Multivariate Analysis of Variance (ANOVA)

was conducted. Significant differences were found in the correlation between BCVA and Choroidal Vascular Area across the three groups (p < 0.001). Given this important difference, Spearman's correlation coefficient was used to assess the correlation between BCVA and Choroidal Vascular Area (r = 0.100; p = 0.311). These two variables' correlations were not statistically significant (Annex 6).

5.6. Post-hoc Power Analysis and Effect Size Results

Due to a small sample size, a Post-hoc Power Analysis and Effect Size Results were performed to assess the adequacy of statistical power to detect clinically meaningful differences in the main metrics of the study.

Table 4 demonstrates that GCC thickness and retina thickness had adequate statistical power (>80 %), ensuring the reliability of detecting clinically meaningful differences with a very low risk of Type II error. Significant differences were observed across the three-group comparisons for these metrics.

In contrast, metrics such as choroid area, choroid vascular area, and CVI exhibited moderate to low statistical power, indicating a higher likelihood of Type II error for these variables. These findings underscore the potential limitations in detecting smaller effect sizes or differences in these metrics.

6. Discussion

Several studies have recognised key OCT-based imaging biomarkers as crucial for the monitoring and prognostication of DME, including disorganisation of the retinal inner layers (DRIL), integrity of the ellipsoid zone (EZ) and external limiting membrane (ELM), the morphology and localisation of intraretinal cysts, and the presence of subretinal fluid (SRF) [20]. Despite these advances, the mechanisms underlying the variability in therapeutic response to AVEGF treatment remain incompletely understood.

Building upon previous findings regarding the differential expression of DNA methyltransferases (DNMTs) in this population [11], the present study aimed to characterise the anatomical profile of the GCC and choroidal parameters (thickness, total and luminal areas, and CVI) in patients with distinct AVEGF treatment response patterns.

The integrity of the GCC of the retina is crucial for visual function maintenance, and its thickness may reflect diverse pathophysiological behaviors. Reasons for GCC thinning can include vascular changes, primary neural degeneration, ischemia, or toxic effects of intravitreal treatments [16]. In the study by Emine Ciloglu et al., a reduction in GCL thickness was observed post-AVEGF treatment, alongside diabetic macular edema regression and BCVA improvement [32]. However, in several patients, no BCVA improvement was observed even after macular thickness normalization, possibly indicating ongoing neurodegenerative processes post-DME resolution [4].

Although the profile of GCL in cases of DMEp is not fully understood,

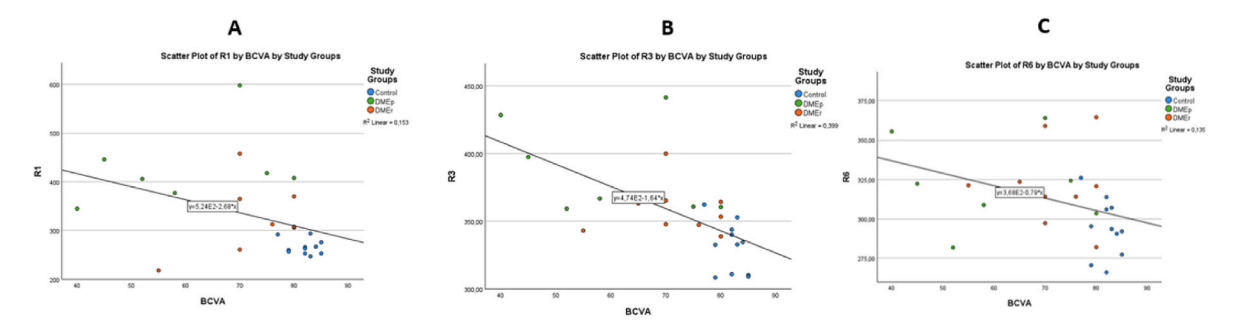


Fig. 3. Scatter plots of linear regression between BCVA and average retinal thickness (1 mm, 3 mm, and 6 mm).

Legend: Control = Control Group; DMEp = Non-responder Group; DMEr = Responder Group; BCVA = Best Corrected Visual Acuity; R1 = Average Retinal Thickness (1 mm); R3 = Average Retinal Thickness (3 mm); R6 = Average Retinal Thickness (6 mm). Fig. 3 illustrates the simple linear regression between BCVA and Average Retinal Thickness in different sectors (A - 1 mm; B - 3 mm; C - 6 mm).

Table 4Post-hoc Power Analysis and Effect Size Results into main retinal variables.

Main retinal variables	Effect Size (Cohen's d)	Statistical Power $(1-\beta)$	Mean Difference (Δ) Control vs. DMEr	Mean Difference (Δ) Control vs. DMEp	Mean Difference (Δ) rDME vs. pDME
GCC Thickness	1.80 (Large effect size)	99.6 %	4.7 <i>p</i> < 0.001	10.8 <i>p</i> < 0.001	6.1 p = 0.002
Retina Thickness	1.89 (Large effect size)	99.8 %	61.9 p = 0.01	$162.1 \ p < 0.001$	100.2 p = 0.04
Choroid Area	0.99 (Large effect size)	71.7 %	-7.4 p = 0.05	-3.4 p = 0.08	4.0 p = 0.12
Choroid Vascular Area	0.80 (Moderate-to-large effect size)	53.2 %	$4.1 \; p = 0.067$	2.4 p = 0.156	-1.7 p = 0.315
Choroidal Vascularity Index	1.01 (Large effect size)	73.4 %	6.0 p = 0.034	5.0 p = 0.065	-1.0 p = 0.438

Legend: GCC = Ganglion Cell Complex; DMEr = Diabetic Macular Edema responder; DMEp = Persistent Diabetic Macular Edema. Values are based on ANOVA for overall comparisons and post-hoc pairwise comparisons using Cohen's dd for effect size. Power was calculated using the non-centrality parameter for the F-distribution. Pairwise differences (Δ) represent the mean difference between groups, with pp-values adjusted using the Tukey method. Statistical analyses were performed using SPSS for ANOVA and post-hoc tests, and Python (SciPy library) for effect size and power calculations ($\alpha = 0.05$).

the study by Lange et al. shows a negative correlation between the severity of retinal ischemia and GCL. Conversely, no correlation was found between GCL and the degree of DME, suggesting GCL may be more relevant in ischemic diabetic retinopathy cases [33].

In this study, the DMEp group exhibited increased GCC thickness at 1 mm ETDRS (p = 0.03), with significant differences noted between the Control Group and the DMEr Group (p = 0.042), and between the Control Group and the DMEp Group (p < 0.01). A structure–function analysis revealed a moderate negative correlation between BCVA and central GCC thickness (r = -0.515; p = 0.03), suggesting that GCC measurements in the central 1 mm may be clinically relevant for predicting visual outcomes post-treatment. From a pathophysiological perspective, diabetic retinopathy involves two parallel mechanisms-vascular dysfunction and neurodegeneration-driven by inflammation, oxidative stress, and breakdown of the blood-retinal barrier. These processes predominantly affect the inner retinal layers, where ganglion cells reside, and are associated with poor visual prognosis. Increased GCC thickness in the DMEp group may reflect early neuroinflammatory responses, including glial cell activation and intracellular edema [16]. Moreover, structural biomarkers such as DRIL often centered in the 1 mm zone, have been strongly linked to worse visual outcomes in DME patients undergoing AVEGF therapy [22]. Overall, the greater sensitivity of the central 1 mm ETDRS subfield may be explained by the thinner baseline GCC in this region, making it more responsive to small pathological changes, as has also been reported in analogous situations with CRT [24].

DME involves macular thickening due to vascular permeability changes [22]. In this regard, Bonnin Sofia et al.'s study supports the hypothesis that the correlation between central macular thickness and BCVA in DME is low [16]. However, Wang Patrick et al.'s systematic review establishes a significant correlation between macular thickness and BCVA in DME patients undergoing AVEGF treatment.

In our study, a negative correlation was found between Retinal Thickness and BCVA at 1 mm ETDRS (p < 0.01), 3 mm ETDRS (p < 0.01), and 6 mm ETDRS (p < 0.01). Spearman's correlation test revealed a negative correlation between Retinal Thickness (1 mm, 3 mm, and 6 mm) and BCVA.

Interestingly, different patterns of DME, as assessed by structural OCT, were associated with varying degrees of neurodegeneration in the inner retinal layers (from the inner margin of the nerve fiber layer to the inner boundary of the outer plexiform layer) and outer retinal layers (from the inner boundary of the outer plexiform layer to the inner margin of the retinal pigment epithelium) [27].

Choroidal segmentation remains a challenging topic due to the lack of reliable automated methods, which necessitates manual intervention [25]. Following a previously published protocol, we achieved excellent interobserver agreement (ICC), although the 6-mm ETDRS sector showed comparatively lower values. (Supplementary Material 7). Regarding the significance of the choroid in the context of DME, findings are not unanimous, with some authors suggesting a significant decrease

in choroidal thickness in DME patients, indicative of an ischemic origin [17]. Other studies report increased choroidal thickness, pointing towards an inflammatory mechanism mediated by VEGF and other cytokines [17], as persistent hyperglycemia activates various pathogenic pathways, including the polyol pathway, hexosamine pathway, protein kinase activation, and advanced glycation end-products regulation (AGES) [2,14]. These mechanisms foster chronic inflammation associated with thickening of the basement membrane, loss of pericytes, and endothelial cell loss, compromising vascular permeability [2,3,9,14].

Udaondo Patricia et al.'s study further suggests a decrease in choroidal thickness in response to AVEGF treatment but indicates it cannot be used as a predictor of response [17].

This study highlights that choroidal thickness at 1 mm in the Control Group (287.0 \pm 143.9 $\mu m)$ is more significant than in the DMEr Group (221.7 \pm 66.3 $\mu m)$ and DMEp Group (214.7 \pm 71.8 $\mu m). At 3 mm, although choroidal thickness is greater in the Control Group (286.5 <math display="inline">\pm$ 139.8 $\mu m)$ compared to the other groups, the DMEr Group (227.6 \pm 65.7 $\mu m)$ exhibits lower thickness compared to the DMEp Group (236.8 \pm 42.1 $\mu m)$. Finally, in the 6 mm region, thickness is highest in the Control Group (260.4 \pm 114.1 $\mu m)$, followed by the DMEp Group (213.6 \pm 40.2 $\mu m)$ and DMEr Group (206.9 \pm 60.2 $\mu m)$. However, these differences are not statistically significant.

The choroidal vasculature plays a critical role in supplying oxygen and nutrients to the metabolically active photoreceptors of the outer retina. Damage to the choroidal vasculature can result in significant retinal dysfunction and impaired visual recovery [18]. The CVI quantifies the ratio of the luminal area to the total choroidal area, providing a detailed assessment of the vascular and stromal components [34]. In diabetic patients, microvascular alterations such as thickened basement membranes, lumen narrowing, and arteriosclerotic changes in choroidal arteries may affect the choroid [35].

The complexity of studying the choroid increases when additional variables, such as DME and treatment, are considered [36]. For example, the DMEp group in our study, likely characterized by elevated VEGF and inflammatory factors, may experience choroidal vessel hyperpermeability [37], contributing to increased choroidal thickness compared to the DMEr group, which exhibited less choroidal thickness [38]. These findings underscore the importance of evaluating choroidal parameters in this context.

In Dou Ningxin et al.'s study, CVI calculated within the central subfoveal 1.5 mm region was a strong predictor of therapeutic response, with DME patients exhibiting higher CVI being more likely to respond to treatment [18]. In our study, significant differences in total choroidal area were observed between the Control and DMEr groups (p = 0.006) and between the DMEr and DMEp groups (p = 0.024). Similarly, significant differences in choroidal vascular area were found between the Control and DMEr groups (p = 0.012) and the DMEr and DMEp groups (p = 0.031). However, CVI in the DMEp group was lower but did not reach statistical significance.

The Spearman correlation analysis revealed a near-significant

positive correlation between BCVA and CVI (p = 0.057), suggesting that a larger sample size might uncover statistically robust relationships. Unlike prior studies that focused on the central 1 mm region, CVI in our study was calculated across the entire horizontal choroidal B-scan, which may have diluted the ability to detect localized differences. These findings imply that the central 1 mm region may hold greater predictive value for treatment response, while broader calculations may not be as sensitive.

Interestingly, although all choroidal metrics were obtained from the same EDI B-scan, significant differences in total and luminal areas were observed without corresponding changes in choroidal thickness. This discrepancy reflects the distinction between linear thickness and structural composition: while thickness measures distance, area-based metrics and CVI capture vascular and stromal distribution. CVI may therefore provide greater sensitivity to subtle choroidal alterations in diabetic patients, especially given that choroidal thickness can increase or decrease depending on disease stage and treatment status [17].

Future studies should adopt a longitudinal approach to assess CVI and choroidal thickness changes before, during, and after treatment. Such an approach would provide insights into the temporal dynamics of these parameters and their utility in monitoring treatment response. Additionally, investigating the relevance of calculating CVI for the entire choroidal area across all 49 OCT scans, rather than a single foveacentered B-scan, may clarify its role in predicting functional and anatomical outcomes.

This study has several limitations that should be considered when interpreting the results. Firstly, although the patient cohort was representative, the relatively small sample size of 27 participants divided into three groups may have limited the statistical power to detect significant differences between groups. This increases the risk of Type II errors and reduces the generalizability of the findings to a broader population.

Post-hoc power analysis revealed adequate power (>80 %) for GCC thickness and retina thickness, ensuring reliability in detecting clinically meaningful differences for these metrics. However, metrics such as choroid area (moderate power), choroid vascular area (low power), and CVI (moderate power) require cautious interpretation due to the potential for Type II errors. These findings highlight the need for larger sample sizes in future studies to ensure adequate power across all metrics, particularly for those with moderate to low power in this study. Expanding the sample size would improve the study's robustness and generalizability, thereby enhancing confidence in detecting clinically meaningful differences for all evaluated metrics.

Secondly, the control group consisted of diabetic patients with no or early-stage DR, while the DME groups presented more advanced DR stages. Although DR severity is known to independently influence choroidal thickness and CVI, the DR severity within the DME subgroups was comparable, and the primary aim of the study was to assess anatomical differences associated with therapeutic response rather than DR stage itself.

Thirthly, the cross-sectional design of this study limits the ability to observe dynamic changes in layer thickness before, during, and after treatment, thereby restricting insights into temporal or causal relationships. This limitation precludes determining whether the observed variations predict therapeutic outcomes or merely reflect treatment effects. To address this, future research should adopt a longitudinal design to enable the prospective collection of data across multiple time points, providing a deeper understanding of these parameters' temporal dynamics and predictive value.

Finally, the subjective component inherent to the measurement process highlights the need to continue assessing and improving reproducibility to ensure measurement reliability. While expert review was performed to minimize segmentation and decentration errors, the semi-automatic and manual corrections introduce the potential for variability and bias. Future studies should apply ocular magnification corrections based on axial length and refractive error when appropriate, and adopt standardised, masked protocols to minimize measurement variability.

Moreover, the integration of advanced algorithmic approaches—particularly those leveraging artificial intelligence (AI)—may enable fully automated and reproducible quantification of GCC and CVI. This would facilitate the analysis of multiple B-scans across the macular volume, thereby capturing topographic variability more comprehensively than single-scan approaches. Incorporating these technological advancements would enhance the robustness of future findings and strengthen their clinical applicability and generalizability.

7. Conclusion

In this study, significant differences were observed in the GCC thickness at 1 mm between the Control Group and DME responders and between the Control Group and Patients with persistent DME The DMEp group exhibited the most significant thickness, which may be attributed to inflammatory processes and the presence of macular edema associated with early activation of glial cells [16]. A moderate negative correlation was observed between BCVA and 1 mm GCC thickness. These findings suggest that 1 mm GCC thickness could be an interesting parameter for predicting visual outcomes after treatment. However, a study by Lange, J. et al. found a negative correlation between the severity of retinal ischemia and GCL thickness. Conversely, no correlation was found between GCC thickness and the severity of DME. These results suggest that GCC thinning may be more relevant in the context of ischemic diabetic retinopathy [33], even in subclinical cases, as a potential indicator of underlying neurodegenerative processe.

The current study observed a negative correlation between retinal thickness (1 mm, 3 mm, and 6 mm) and BCVA. These findings align with those reported in the systematic review by Wang, Patrick et al., which demonstrated a significant correlation between macular thickness and BCVA in DME patients undergoing AVEGF treatment [26].

Regarding the importance of the choroid in this context, findings are not unanimous, as the choroidal state in diabetic patients is highly variable, even among patients classified with the same ETDRS level [17]. Indeed, choroidal thickness before treatment may be increased or decreased depending on the underlying pathogenic mechanism [17]. In our study, we did not observe statistically significant differences in choroidal thickness between the studied groups. Therefore, future studies should consider choroidal analysis before, during, and after treatment, as variations in thickness may serve as a valuable indicator for monitoring therapeutic response rather than a direct predictor.

Finally, statistically significant differences were found in the analyses of the total choroidal area and the vascular area between the DMEp and DMEr groups. However, the CVI did not reach statistical significance. The Spearman correlation analysis between BCVA and CVI suggests that a larger sample size could reveal statistically significant associations. This study may provide future insights into the relevance of calculating CVI for the total choroidal area and its impact on functional gain.

CRediT authorship contribution statement

Ana Condelipes: Writing – review & editing, Writing – original draft, Validation, Software, Investigation, Conceptualization. Daniela Correia: Software, Methodology, Investigation, Conceptualization. Inês Fernandes: Writing – review & editing, Writing – original draft, Software, Methodology, Investigation, Conceptualization. Tiago Silva: Software, Methodology, Investigation, Conceptualization. Eduardo Correia: Software, Methodology, Bruno Pereira: Supervision, Methodology, Investigation. Pedro Camacho: Supervision, Project administration, Methodology, Investigation, Funding acquisition.

Ethics approval and consent to participate

The research protocol was approved from each Institutional Ethical Review Board before study start (IDI&CA-IPL_CE-ESTeSL-

N°0.08–2021), and all of the patients provided signed informed consent.

Ethics statement

This study, titled "Thickness Profile of the Ganglion Cell Complex and Choroid in Patients with Persistent Diabetic Macular Edema," complies with relevant laws and institutional guidelines. The research protocol was reviewed and approved by the Institutional Ethical Review Board (IDI&CA-IPL_CE-ESTeSL-N°0.08–2021) before the study began. All procedures adhered to the principles outlined in the Declaration of Helsinki. Participants provided written informed consent before enrollment, and their privacy and confidentiality rights were rigorously protected.

Additionally, this material is the authors' original work, which has not been previously published elsewhere, and the paper is not currently under consideration for publication elsewhere. It reflects the authors' own research and analysis in a truthful and complete manner, and all meaningful contributions of co-authors and co-researchers have been properly credited. The results are appropriately contextualized within prior and existing research, and all sources used have been fully disclosed and correctly cited, with direct quotations clearly indicated.

Funding acquisition

This project was partially supported by an IDI&CA grant IPL/2021/DiffMeDiME_ESTeSL, by H&TRC- Health & Technology Research Center, ESTeSL- Escola Superior de Tecnologia da Saúde, Instituto Politécnico de Lisboa, FCT/MCTES national support through the UIDP/05608/2020 (https://doi.org/10.54499/UIDP/05608/2020), UIDB/05608/2020 (https://doi.org/10.54499/UIDB/05608/2020) and by Retina Institute of Lisbon (IRL).

All authors have read and agreed to the published version of the manuscript.

Declaration of competing interest

The authors declare the following financial interests/personal relationships which may be considered as potential competing interests: Pedro Camacho reports financial support was provided by Lisbon Polytechnic Institute Lisbon School of Health Technology. If there are other authors, they declare that they have no known competing financial interests or personal relationships that could have appeared to influence the work reported in this paper.

Acknowledgments

This project was partially supported by an IDI&CA grant IPL/2021/DiffMeDiME_ESTeSL, by H&TRC- Health & Technology Research Center, ESTeSL- Escola Superior de Tecnologia da Saúde, Instituto Politécnico de Lisboa, FCT/MCTES national support through the UIDP/05608/2020 (https://doi.org/10.54499/UIDP/05608/2020), and UIDB/05608/2020 (https://doi.org/10.54499/UIDB/05608/2020) and by Retina Institute of Lisbon (IRL).

Appendix A. Supplementary data

Supplementary data to this article can be found online at https://doi.org/10.1016/j.compbiomed.2025.111192.

References

- [1] J. Zhang, C. Zhang, L. Gu, D. Luo, Q. Qiu, J. Zhang, J. Zhang, C. Zhang, J. Zhang, L. Gu, D. Luo, Q. Qiu, Diabetic macular edema: current understanding, molecular mechanisms and therapeutic implications, Citation, https://doi.org/10.3390/cell s11213362, 2022.
- [2] V. Starace, M. Battista, M. Brambati, M. Cavalleri, F. Bertuzzi, A. Amato, R. Lattanzio, F. Bandello, M.V. Cicinelli, The role of inflammation and

- neurodegeneration in diabetic macular edema, Ther Adv Ophthalmol 13 (2021), https://doi.org/10.1177/25158414211055963.
- [3] G.T. Xu Tang, J.F. Zang, Inflammation in diabetic retinopathy: possible roles in pathogenesis and potential implications for therapy, Neural Regen Res (2023), https://doi.org/10.4103/1673-5374.355743.
- [4] X. Li, C. Li, H. Huang, D. Bai, J. Wang, A. Chen, Y. Gong, Y. Leng, Anti-vascular endothelial growth factor drugs combined with laser photocoagulation maintain retinal ganglion cell integrity in patients with diabetic macular edema: study protocol for a prospective, non-randomized, controlled clinical trial, Neural Regen Res 19 (2024) 923–928, https://doi.org/10.4103/1673-5374.382104.
- [5] D. Akira Kondo Kuroiwa, Fernando Korn Malerbi, Caio Vinicius Saito Regatieri, D. Akira Kondo Kuroiwa, New insights in resistant diabetic macular edema, Ophthalmologica 244 (2021) 485–494, https://doi.org/10.1159/000516614.
- [6] W. Wang, A.C.Y. Lo, Molecular sciences diabetic retinopathy: pathophysiology and treatments, (n.d.). https://doi.org/10.3390/ijms19061816.
- [7] D. Soni, P. Sagar, B. Takkar, Diabetic retinal neurodegeneration as a form of diabetic retinopathy, Int. Ophthalmol. 41 (2021) 3223–3248, https://doi.org/ 10.1007/s10792-021-01864-4.
- [8] Diagnosis and classification of diabetes mellitus. https://doi.org/10.2337/dc11-S062, 2011.
- [9] Y.-M. Kuo, S.F. Abcouwer, G. Casini, A. Francisco Ambrósio, J. Zhang, A. Arrigo, B. M. Parodi, L. Bianco, E. Aragona, A. Antropoli, A. Berni, A. Saladino, M. Battaglia Parodi, F. Bandello, Neuroinflammation and neurodegeneration in diabetic retinopathy. https://doi.org/10.3389/fnagi.2022.937999, 2022.
- [10] E. Garcia-Martin, M. Cipres, I. Melchor, L. Gil-Arribas, E. Vilades, V. Polo, M. J. Rodrigo, M. Satue, Neurodegeneration in patients with type 2 DiabetesMellitus without diabetic retinopathy. https://doi.org/10.1155/2019/1825819, 2019.
- [11] P. Camacho, E. Ribeiro, B. Pereira, T. Varandas, J. Nascimento, J. Henriques, M. Dutra-Medeiros, M. Delgadinho, K. Oliveira, C. Silva, M. Brito, DNA methyltransferase expression (DNMT1, DNMT3a and DNMT3b) as a potential biomarker for anti-VEGF diabetic macular edema response, Eur. J. Ophthalmol. 33 (2023) 2267–2274, https://doi.org/10.1177/11206721231171623.
- [12] E. Hee Hong, H. Yeom, H. Seon Yu, J. Eun Park, Y. Un Shin, S.-Y. Bang, H. Cho, Genome-wide association study of the response of patients with diabetic macular edema to intravitreal Anti-VEGF injection, Sci. Rep. | 12 (123AD) 22527. htt ps://doi.org/10.1038/s41598-022-26048-7..
- [13] X. Du, L. Yang, L. Kong, Y. Sun, K. Shen, Y. Cai, H. Sun, B. Zhang, S. Guo, A. Zhang, X. Wang, P. Yin, W. Dai, Y. Ouyang, Metabolomics of various samples advancing biomarker discovery and pathogenesis elucidation for diabetic retinopathy, Front. Endocrinol. 13 (2022) 1037164, https://doi.org/10.3389/fendo.2022.1037164. OPEN ACCESS EDITED BY.
- [14] R. Simó, O. Simó-Servat, P. Bogdanov, C. Hernández, Diabetic retinopathy: role of neurodegeneration and therapeutic perspectives, Asia-Pacific Journal of Ophthalmology 11 (2022) 160–167, https://doi.org/10.1097/ APO.000000000000010.
- [15] A. Markan, A. Agarwal, A. Arora, K. Bazgain, V. Rana, V. Gupta, Novel imaging biomarkers in diabetic retinopathy and diabetic macular edema, Ther Adv Ophthalmol 12 (2020) 251584142095051, https://doi.org/10.1177/ 2515841420950513.
- [16] S. Bonnin, R. Tadayoni, A. Erginay, P. Massin, B. Dupas, Correlation between ganglion cell layer thinning and poor visual function after resolution of diabetic macular edema, Investig. Ophthalmol. Vis. Sci. 56 (2015) 978–982, https://doi. org/10.1167/joys.14-15503
- [17] P. Udaondo Mirete, C. Muñoz-Morata, C. Albarrán-Diego, E. España-Gregori, Influence of intravitreal therapy on choroidal thickness in patients with diabetic macular edema, J. Clin. Med. 12 (2023) 348, https://doi.org/10.3390/ jcm12010348.
- [18] N. Dou, S. Yu, C.-K. Tsui, B. Yang, J. Lin, X. Lu, Y. Xu, B. Wu, J. Zhao, X. Liang, Choroidal vascularity index as a biomarker for visual response to antivascular endothelial growth factor treatment in diabetic macular edema. https://doi.org/1 0.1155/2021/3033219, 2021.
- [19] O. Akmaz, G. Tokac, M. Garli, M. Cetin, M. Karatas, Y.Z. Guven, B. Yuksel, T. Kusbeci, Vascular indexes of choroidal layers in diabetic macular edema, (n.d.). https://doi.org/10.14744/eer.2024.42275.
- [20] G. Panozzo, M.V. Cicinelli, A.J. Augustin, M. Battaglia Parodi, J. Cunha-Vaz, G. Guarnaccia, L. Kodjikian, L.M. Jampol, A. Jünemann, P. Lanzetta, A. Löwenstein, E. Midena, R. Navarro, G. Querques, F. Ricci, U. Schmidt-Erfurth, R. M. da Silva, S. Sivaprasad, M. Varano, G. Virgili, F. Bandello, An optical coherence tomography-based grading of diabetic maculopathy proposed by an international expert panel: the european school for advanced studies in ophthalmology classification, Eur. J. Ophthalmol. 30 (2020) 8–18, https://doi.org/10.1177/
- [21] S.S. Dabir, D. Das, J. Nallathambi, S. Mangalesh, N.K. Yadav, J.S.A.G. Schouten, Differential systemic gene expression profile in patients with diabetic macular edema: responders versus nonresponders to standard treatment, Indian J. Ophthalmol. (2014) 66–73, https://doi.org/10.4103/0301-4738.126186.
- [22] O.A. Sorour, E.S. Levine, C.R. Baumal, A.G. Elnahry, P. Braun, J. Girgis, N. K. Waheed, Persistent diabetic macular edema: definition, incidence, biomarkers, and treatment methods, Surv. Ophthalmol. 68 (2023) 147–174, https://doi.org/10.1016/j.survophthal.2022.11.008.
- [23] M. Parravano, E. Costanzo, G. Querques, Profile of non-responder and late responder patients treated for diabetic macular edema: systemic and ocular factors, Acta Diabetol. 57 (2020) 911–921, https://doi.org/10.1007/s00592-020-01496-7.
- 24] M. Pazos, A.A. Dyrda, M. Biarnés, A. Gómez, C. Martín, C. Mora, G. Fatti, A. Antón, Diagnostic accuracy of spectralis SD OCT automated macular layers segmentation

- to discriminate normal from early glaucomatous eyes, Ophthalmology 124 (2017) 1218–1228, https://doi.org/10.1016/j.ophtha.2017.03.044.
- [25] M. Zhao, D. Alonso-caneiro, R. Lee, A.M.Y. Cheong, W. Yu, H. Wong, A.K.C. Lam, Comparison of choroidal thickness measurements using semiautomated and manual segmentation methods, Optometry. Vision. Sci. 97 (2020) 121–127, https://doi.org/10.1097/OPX.000000000001473.
- [26] P. Wang, Z. Hu, M. Hou, P.A. Norman, E.K. Chin, D.R.P. Almeida, Relationship between macular thickness and visual acuity in the treatment of diabetic macular edema with Anti-VEGF therapy: systematic review, J Vitreoretin Dis 7 (2023) 57–64, https://doi.org/10.1177/24741264221138722.
- [27] E. Borrelli, C. Barresi, A. Feo, G. Lari, D. Grosso, L. Querques, R. Sacconi, F. Bandello, G. Querques, Imaging biomarkers and clinical factors associated with the rate of progressive inner and outer retinal thinning in patients with diabetic macular edema, Sci. Rep. 13 (2023), https://doi.org/10.1038/s41598-023-30432-2.
- [28] P. Camacho, M. Dutra-Medeiros, L. Salgueiro, S. Sadio, P.C. Rosa, Manual segmentation of 12 layers of the retina and choroid through SD-OCT in intermediate AMD: repeatability and reproducibility, J. Ophthalmic Vis. Res. 16 (2021), https://doi.org/10.18502/jovr.v16i3.9435.
- [29] S. Sonoda, T. Sakamoto, T. Yamashita, M. Shirasawa, E. Uchino, H. Terasaki, M. Tomita, Choroidal structure in normal eyes and after photodynamic therapy determined by binarization of optical coherence tomographic images, Investig. Ophthalmol. Vis. Sci. 55 (2014) 3893–3898, https://doi.org/10.1167/iovs.14-14447.
- [30] K. Khurshid, I. Siddiqi, C. Faure, N. Vincent, Comparison of niblack inspired binarization methods for ancient documents, in: Document Recognition and Retrieval XVI, SPIE, 2009, p. 72470U, https://doi.org/10.1117/12.805827.
- [31] R. Agrawal, P. Gupta, K.A. Tan, C.M.G. Cheung, T.Y. Wong, C.Y. Cheng, Choroidal vascularity index as a measure of vascular status of the choroid: measurements in

- healthy eyes from a population-based study, Sci. Rep. 6 (2016), https://doi.org/10.1038/srep21090.
- [32] E. Ciloglu, F. Unal, N.C. Dogan, Changes in the ganglion cell complex thickness after anti-VEGF treatment for diabetic macular edema, Arq. Bras. Oftalmol. 83 (2020), https://doi.org/10.5935/0004-2749.20200045.
- [33] J. Lange, M. Hadziahmetovic, J. Zhang, W. Li, Region-specific ischemia, neovascularization and macular oedema in treatment-naïve proliferative diabetic retinopathy, Clin. Exp. Ophthalmol. 46 (2018) 757–766, https://doi.org/10.1111/ ceo.13168.
- [34] S. Subramaniyan, V. Perumal, J. Balachandar, Choroidal thickness and choroidal vascularity index in diabetic retinopathy and diabetic macular edema – a clinical study, TNOA Journal of Ophthalmic Science and Research 60 (2022) 254, https://doi.org/10.4103/tjosr.tjosr_18_22.
- [35] M. Motamed Shariati, S. Khazaei, M. Yaghoobi, Choroidal vascularity index in health and systemic diseases: a systematic review, Int J Retina Vitreous 10 (2024), https://doi.org/10.1186/s40942-024-00607-8.
- [36] Y. Chen, H. Xian, M. Liu, X. Dong, S. Du, Regional assessment of choroidal vascularity index in patients with pre- and early-stage diabetic retinopathy using ultra-wide-field OCTA, Front. Med. 11 (2024), https://doi.org/10.3389/ fmed.2024.1490831.
- [37] S.Y. Peng, T.C. Chen, Y.T. Hsieh, T.C. Ho, C.M. Yang, C.H. Yang, Choroidal changes in patients with diabetic retinopathy: a retrospective study, Diagnostics 14 (2024), https://doi.org/10.3390/diagnostics14050537.
- [38] F. Savur, H. Kaldırım, K. Atalay, T. Öğreden, Ş.Ç. Hayat, Treatment results of diabetic macular edema with different choroidal thickness with intravitreal anti vascular endothelial growth factor, BMC Ophthalmol. 22 (2022), https://doi.org/ 10.1186/s12886-022-02721-3.